Excavation Autonomy with Resilient Traversability and Handling

Yash Turkar†, Sugheerth Sreedharan†, Christo Aluckal†, Ishaan Malhotra†, Roopesh Vinod Kumar Lal†, Jainam Jain†, Yashom Dighe†, Youngjin Kim†, Jake Gemerek◇, Karthik Dantu†

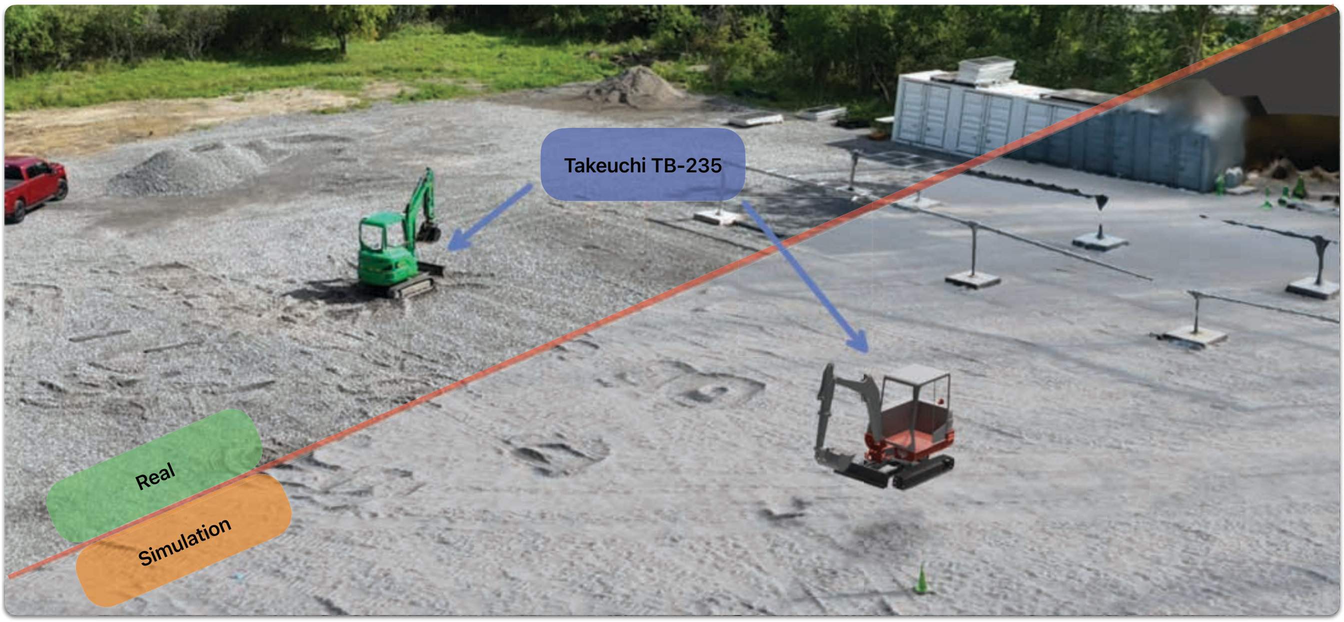

Fig. 1: EARTH introduces an excavation autonomy framework with a focus on formal safety and robust perception. Figure shows our autonomous Takeuchi TB-235 excavator in real-world and simulated environments. Our simulator, TERA, supports realistic soil and deformation models.

***Abstract*— The construction industry faces significant challenges due to workforce shortages and the need for increased safety and productivity. Autonomous excavators and construction machinery offer a promising solution leveraging recent advances in autonomy. However, deploying large autonomous machines presents unique hurdles in areas such as safe planning and control, reliable state estimation, and robust perception in dynamic environments. This paper introduces EARTH, a framework designed to enable the autonomy for excavators. We detail the EARTH platform architecture, identify key challenges inherent in autonomous excavation, and propose potential solutions. Preliminary results demonstrating the effectiveness of our approach are presented, along with a discussion outlining future research directions to advance autonomous construction and excavation.**

I. Introduction

Autonomous robotics has been a promising solution to mitigate risks to human workers by operating in dangerous conditions while simultaneously increasing productivity through continuous operation and precise execution. Mobile robots equipped with robotic manipulators help pre/post fabrication [1], UAVs facilitate inspection and monitoring [2] and exoskeletons to reduce effort [3], Despite these advances, the adoption of autonomous systems in the field is limited due to lack of safe and generalizable algorithms, and uncertainty in environments. Incorporating autonomy into large machines such as excavators requires increase reliability as it operates under extreme environments and can cause catastrophic failures.

Although full-size excavators have been previously explored in prior work ([4], [5]), significant challenges remain in adapting autonomous systems to these large, complex, hydraulic machines. First, pose estimation of the excavator end-effector is difficult due to limited sensing, perception occlusion and noisy measurements. Second, increased size of actuators and non-linear response of hydraulics increases complexity in control. Third, given the potential for significant damage in case of collisions, safety in motion planning is critical. Finally, current simulation environments supporting these machines and deformable terrain are limited. To address these challenges, we propose the EARTH[1] (Excavation Autonomy with Resilient Traversability and Handling) framework, an autonomy solution with specific emphasis on excavation autonomy. Our contributions are as follows:

1) Introduce a software-stack for autonomous excavators

Authors † are with the Department of Computer Science and Engineering, University at Buffalo, Buffalo, NY 14260, USA. Author ◇ is with MOOG Inc. This project is supported by a grant from MOOG Inc. {yashturk,...,kdantu}@buffalo.edu

[1] https://github.com/droneslab/EARTH

based on the perception-estimation-planning-control paradigm comprising several customizable modules
2) Propose a simulation environment comprising a Takeuchi TB-235 excavator and deformable terrain capabilities
3) Novel manipulator pose-estimation with hydraulic pressure and inertial sensing
4) A safety-focused planning method based on control barrier and lyapunov functions

II. Excavation Autonomy Stack

Figure 3 illustrates our excavation stack, the software architecture enabling autonomy on our Takeuchi TB-235 excavator. The stack follows the perception-estimation-planning-control paradigm [6] with a focus on modularity and safety. The stack contains the following modules :

Sensing: The sensing module is responsible for interfacing with a variety of sensors. These include LiDARs, cameras, inertial measurement units (IMUs), hydraulic pressure transducers, geartooth encoders (for cab position), and GNSS receivers. Precise time synchronization is achieved through hardware clock sync for the LiDARs and cameras, while other sensors rely on ROS for time alignment. This coordinated sensor data streams are made available as ROS2 topics for use by other modules.

Estimation: The state-estimation module (described in subsection IV-A) is split into two submodules. The first focuses on **localization and mapping**, accurately determining the excavator's pose within its environment and generating high-resolution maps essential for path planning and task execution. The second submodule specializes in estimating the **joint states and efforts** of the excavator's primary actuators: the boom, arm, bucket, and cab.

Planning: The planning module employs a hierarchical approach, encompassing both global and local path planning through its "**Nav Planner**" components. This planner is responsible for determining optimal routes, considering factors such as terrain deformation, static and dynamic obstacle avoidance, kinematic, and dynamic constraints. The core attribute in achieving autonomous excavation involves manipulator trajectory planning. The "**Manipulator Planner**" module is dedicated to handling the problems associated with manipulator planning, including digging and dumping operations in a safe and efficient manner.

Control: The control module translates the plans generated by the planning module into precise and efficient actions. Structured similarly to the planning module, it comprises two sub-modules: the "**Nav Controller**" and the "**Manipulator Controller**." The Nav Controller governs the excavator's movement by independently commanding appropriate control to each of the tracks that satisfy actuator limits while minimizing actuation delay owing to hydraulic dynamics. Meanwhile, the Manipulator Controller employs an inverse kinematics approach to ensure accurate and coordinated movements of the excavator's boom, arm, and bucket. Furthermore, the controller should be robust to handle disturbances during digging operations and compensate for unmodeled dynamic variations induced by material removal and accumulation during excavation.

Actuation: Mirroring the sensing module's architecture, the actuation module is responsible for interfacing with the excavator's physical hydraulic actuators. Traditional manually operated excavators, such as the TB235-2 [7], employ multiple levers and pedals to control each actuator. In our excavator, we have replaced the physical levers with electronically controllable hardware that communicates using CAN. This interface is provided through a ROS wrapper via the `DeltaCAN` msg, a custom message encapsulating this control scheme. This data structure provides generalizability and can be replicated to other excavator configurations.

Importantly, the estimation, planning, and control modules within the autonomy stack are designed with a modular architecture, ensuring they are hardware and platform agnostic. This means they can operate effectively across diverse physical platforms and seamlessly integrate with simulation environments.

III. Simulation

Developing autonomy algorithms for outdoor tasks such as excavation is extremely challenging. Perception in offroad environments where excavation tasks happen is arguably more challenging than in more structured environments such as roads. Further, task-specific perception involves understanding soil characteristics, detailed terrain models, and full 360° awareness for safety. Motion planning for navigation involves reasoning about obstacles as well as terrain elevations as is the case in most offroad scenarios. Task-based planning requires detailed modeling of hydraulic actuation (typical for excavator arms), contact dynamics with the ground during excavation and understanding of terrain deformation during the task. Finally, control requires precise ability to follow specified plans for safety as well as exact task execution. Developing all these components require detailed testing that is challenging in realistic environments. A method to alleviate this challenge is the use of realistic simulation.

To address the mentioned concerns, we developed TERA[2] [8] (Simulator for Terrain Excavation Robot Autonomy), introducing the following :

1) The first comprehensive simulation environment to study autonomous excavation. TERA allows realistic modeling of perception, planning and control of excavators in realistic environments allowing the study of all aspects of excavation autonomy
2) Built to be customizable and extensible allowing users to import their excavators, environments and excavation tasks easily. With ROS integration, it is easy to quickly integrate existing autonomy modules as well. This allows users to quickly re-create their environment and focus on the development of autonomy algorithms

[2]https://droneslab.github.io/tera/

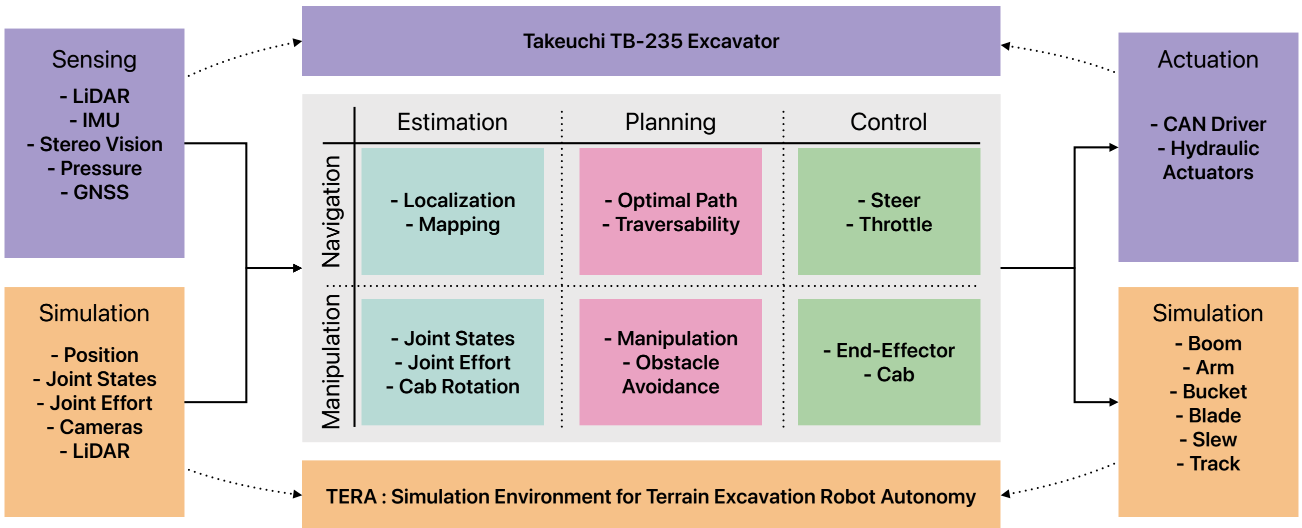

Fig. 3: Illustrates our excavation autonomy stack detailed in section II. Estimation, Planning and Control modules are platform agnostic and work seamlessly on our Takeuchi TB-235 excavator and in TERA, our simulation environment.

3) Using Unity and AGX, TERA is scalable to use multiple excavators while performing high-fidelity simulation including detailed contact physics for excavation in real-time on desktop hardware

A. Overview

TERA offers a highly realistic simulation environment capable of modeling realistic excavators, realistic environments, and their interactions. It uses Unity3D for visualization due to it's powerful graphics rendering and development framework that aid in rapidly developing realistic, efficient and easily deployable simulations. Interactions with the terrain occur using the AGX Dynamics Plugin [9]. The AGX Terrain allows for modeling and simulation of soil deformation via interactions between parts of the robot (tracks, bucket) and the soil. We can model physical properties of the terrain to adapt it to various real life terrains such as soil, gravel, sand, and others.

All communications with the high level application occur using ROS2. Users communicate with the excavator via the custom `DeltaCAN` message. AGX Dynamics performs internal dynamics calculations and updates the state of the excavator components based on the control. In parallel, the sensor information is also computed. Once the simulation step is performed, the new excavator state values and the sensor values are retrieved. These values are wrapped in the desired ROS bindings and provided to the user.

B. Robot Modeling

The excavator model consists of 4 main components - a 4 degree-of-freedom manipulator, the cab, the base and the tracks. The manipulator is mounted on the cab which has the ability to slew freely about the base. The base is rigidly attached to the track mechanism which allows the excavator to move with a non-holonomic differential drive mechanism. This excavator was first modeled in CAD. Each component of the robot was individually modeled. Then, the models were converted to URDFs (Unified Robot Description Format) along with their physical properties such as mass, inertia matrix, stiffness, dampening, friction etc.

C. Terrain Interaction

The terrain interactions are modeled according to [10], where the terrain is divided into multiple granularity levels. Each level involves different calculation complexities, offering a reasonable balance between computational effort and accuracy. When the bucket makes contact with the terrain, the angle made by the cutting edge and the ground is evaluated. Based on the angle of the edge and the terrain shearing properties, the terrain deforms. When the terrain deforms, the excavated soil is converted to dynamic soil particles. These particles interact with other particles, terrain meshes and the excavator itself. The mesh location from which the soil was excavated from now contains a depression indicating the removal of material. Figure 4 shows a digital elevation model view of the simulated terrain after performing digging motion. We can see that deformation is caused by both digging (the bucket interaction with terrain) as well as the motion (track interaction with terrain) of the excavator.

D. Sensor Simulation

Sensors are integrated into TERA's excavators via the Unity Sensors plugin [11]. The sensor suite includes RGB cameras, RGBD cameras, IMUs and LiDARs. Each sensor's internal parameters such as the camera's resolution, IMU acceleration bias/noise, etc. can be defined explicitly.

E. Realistic Actuation

Once the URDF and the 3D Meshes are defined, it can be imported into Unity. Each link in the kinematic chain is

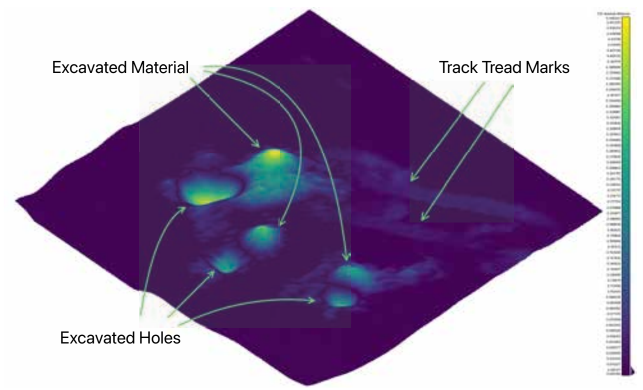

Fig. 4: Elevation model of the terrain after three excavation tasks, showing accurate deformation due to digging. The track-threads from the excavator's traversal are visible, with the elevation model color-coded to highlight the unit changes before and after the experiment.

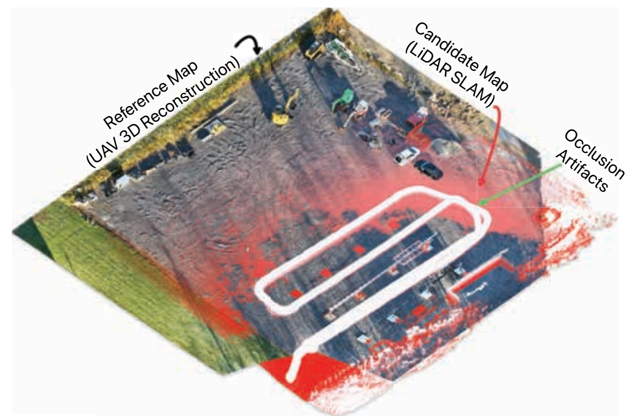

Fig. 5: Red-white point cloud shows 3D map generated using a LiDAR SLAM method. White streak shows artifacts in map due to the body of the excavator mapped into the resulting 3D point cloud. Optimizing sensor placement can mitigate this issue.

defined with it's mass, inertia matrix (in X-Y-Z axis) and joint type. For revolute joints, a hinge constraint is defined between each link as they rotate about their Z axis. The constraint includes capabilities of modeling rotation limits, target speed controllers and friction blocks with defined compliance (stiffness), damping and force limits. A target speed controller is utilized to move the joints. Regardless of the input velocity command, the speed controller reaches the target speed with minimal transient response time. For the purpose of maintaining a model-agnostic nature of the proposed simulator, we allow the lower-level controller to have nearly infinite acceleration, which is hardly achievable in real-world applications. To replicate the motion of a real excavator, we conducted an experimental study where a various range of input signals were commanded and joint velocity was monitored by the onboard inclinometers that provide angular position and velocity with respect to gravity. The actual velocity profiles are parameterized as:

$$\omega^i(t) = \omega^i_{ss}(1 + \sin(\eta^i t + \phi^i)e^{-\beta^i t}) \tag{1}$$

where ω^i_{ss} is the angular velocity of the joint at steady states, obtained from the experimental study and i = [boom, arm, bucket]. The user-selected performance parameters, η^i, β^i and ϕ^i, govern the frequency of oscillation, decay rate and delay, respectively, which can be freely selected based on hardware performance. Using Equation 1, we assign $\eta^i = 20$. $\beta^i = 6$ and $\phi^i = 0$ based on empirical testing.

F. Control

To test the actuation of the tracks and the sim-to-real transfer capability of the simulator, the real excavator was controlled by a conventional joy input. These joystick inputs were recorded and replayed as input to the simulator (via ROS bag). The real excavator was equipped with 2 GPS receivers in a Differential configuration which provides accurate Latitude-Longitude-Altitude upto 0.75m along with heading. The Geodetic co-ordinates were converted to local ENU (Cartesian XYZ) co-ordinates using the Geodetic-ECEF-ENU conversion [12], [13]. The total track length of the real excavator was 57.39m while the length of the simulated excavator was 50.47m with an RMSE of 1.376m between them. Fine-tuning of the terrain parameters based on the real operational parameters could further reduce this gap.

IV. Challenges and Proposed Solutions

A. State Estimation

Accurate state estimation is a fundamental challenge in robotics and autonomous systems, particularly when dealing with complex machinery like excavators. Noisy sensor data, inherent sensing errors, and imprecise system dynamics models can lead to significant estimation drift over time. This issue is further compounded by the use of hydraulic actuators, which often exhibit substantial dead-bands and non-linear control responses. To address these challenges, excavator state estimation is divided into two key sub-modules: localization and mapping, which focuses on accurately determining the excavator's pose within its environment and generating high-resolution maps; and joint state and effort estimation, which specializes in estimating the joint states and efforts of the excavator's primary actuators.

1) Localization and Mapping: Autonomous navigation requires precise odometry, re-localization and high-resolution mapping of the excavator's region-of-operation (ROO). While modern visual and LiDAR SLAM algorithms have advanced significantly and can effectively address a wide range of applications, certain challenges persist in the context of excavation autonomy. Factors such as repeating features in the environment, low and varying light conditions, occlusion from large objects or terrain, and harsh operating environments can degrade SLAM performance. Excavation-specific SLAM methods, such as [insert reference to specific method], have been developed to address these issues and improve localization accuracy. However, reliably fusing data from multiple sensor modalities (e.g., LiDAR, cameras, IMUs) in the presence of occlusion remains an open problem requiring investigation.

We evaluated several SLAM methods such as [14], [15], [16] on our excavator platform. We present our findings and propose solutions.

Sensor Occlusion: We observed that relying on a single LiDAR or camera can be problematic due to occasional occlusion by the excavator's manipulator arm and body. This obstruction hinders the SLAM algorithm's ability to perceive its surroundings effectively, leading to degraded localization accuracy, potential tracking failures and artifacts in the resulting map. While an effective solution to this problem is using multiple sensors [17], occlusion detection and management is crucial. We propose using our previous and on-going work, PIXER [18] and L-DYNO [19], which aid in eliminating unreliable features due to occlusion and motion. Further, the dense maps generated by these SLAM systems can be evaluated using Empir3D [20] for adequate resolution and accuracy.

Global Localization: Achieving reliable global localization for autonomous excavators requires a robust approach that addresses the limitations of individual sensor modalities. While GNSS fusion with SLAM offers a promising solution, it faces challenges such as signal obstructions, multipath errors, and the need for precise time synchronization. To overcome these hurdles, we implemented a real-time fusion system combining LiDAR-Inertial Odometry (LIO) with Real-Time Kinematic (RTK) GNSS. This synergistic approach leverages the global positioning accuracy of RTK GNSS while benefiting from the high-resolution position estimates provided by LIO. Furthermore, we integrated known reference points or ground control points (GCPs) with predefined GNSS coordinates to serve as fiducials for improved localization accuracy within the ROO and consistency across multiple sessions.

Traversability Estimation: Accurate and frequently updated 3D maps are crucial for safe and efficient operation. High-resolution LiDARs coupled with SLAM techniques can generate detailed maps, but artifacts introduced by the excavator itself often hinder traversability estimation. Our preliminary results demonstrate that the excavator arm can appear as a blurred obstacle in the map, misleading the navigation system (see Figure 5). This issue highlights the need for optimized sensor placement to minimize such artifacts and maximize mapping accuracy. We are currently investigating sensor placement optimization using Mixed-integer-linear-programming (MILP) [21]. This approach allows us to systematically explore different sensor configurations on the excavator and identify the optimal location that minimizes mapping errors and improves traversability estimation.

2) Joint State and Effort Estimation: Precise manipulation in autonomous excavators hinges on accurate joint state and effort estimation. Electrically powered manipulators typically rely on motor encoders and controllers for these measurements. However, hydraulic actuators, common in excavators, lack direct measurement capabilities for joint states and efforts, posing a significant challenge. Previous approaches, such as HEAP, have employed draw-wire encoders to measure piston length, which correlates with joint angles. While effective, this method is expensive and susceptible to damage in harsh operating environments. Inertial sensors like IMUs and inclinometers offer an alternative but suffer from drift over time, compromising accuracy.

We present our findings and propose solutions to address these limitations:

Fusion of Inertial Sensing and Hydraulic Pressure: Our approach leverages the pressure transducers on each excavator piston. By studying the relationship between fluid pressure and joint states/efforts, we aim to develop a robust estimation model. Preliminary tests demonstrate a strong correlation between pressure measurements and joint motion, particularly when constrained by payload in the bucket. However, mathematically modeling the relationship between joint torques and pressure values is not feasible due to the many-to-one mapping between values. High pressure can imply high angular velocities of the joint with an unloaded bucket or a slow motion with a loaded bucket. Furthermore, each joint is controlled by two pistons which adds to the complications. Currently, we are working on a data driven approach that fuses inertial sensor readings and the pressure values to output joint angles.

Payload and Effort Estimation: The presence of multiple pressure sensors allows us to jointly estimate not only joint position and effort but also payload weight within the excavator's bucket. This assists downstream applications such as digging and excavation where knowing the amount of unearthed material is important. Preliminary results (Figure 7 show strong spearman correlation between joint angles and hydraulic pressure for different excavator links. We aim to develop a pressure-inclinometer estimation system to accurately track the excavator joints.

An additional challenge lies in evaluating the accuracy of our joint state estimation. Traditional motion capture systems, often used for ground truth pose tracking, face limitations in outdoor scenarios involving large machinery like excavators. To address this, we employ a system utilizing AprilTags [22] (as demonstrated in Figure 6), enabling us to measure the ground truth pose of the excavator's joints. Significant tuning was required in terms of AprilTag size, camera exposure and resolution settings, and frame transformations to engineer a robust ground-truth pose solution capable of handling the complexities of our experimental setup.

B. Safe Planning

Ensuring safe and reliable operation for heavy-duty robots like excavators presents unique challenges in complex environments. While traditional planning approaches often rely on post-hoc collision checking, leaving a margin of uncertainty. This motivates us to explore more formal safe planning methods which contribute to the development of trustworthy autonomous solution.

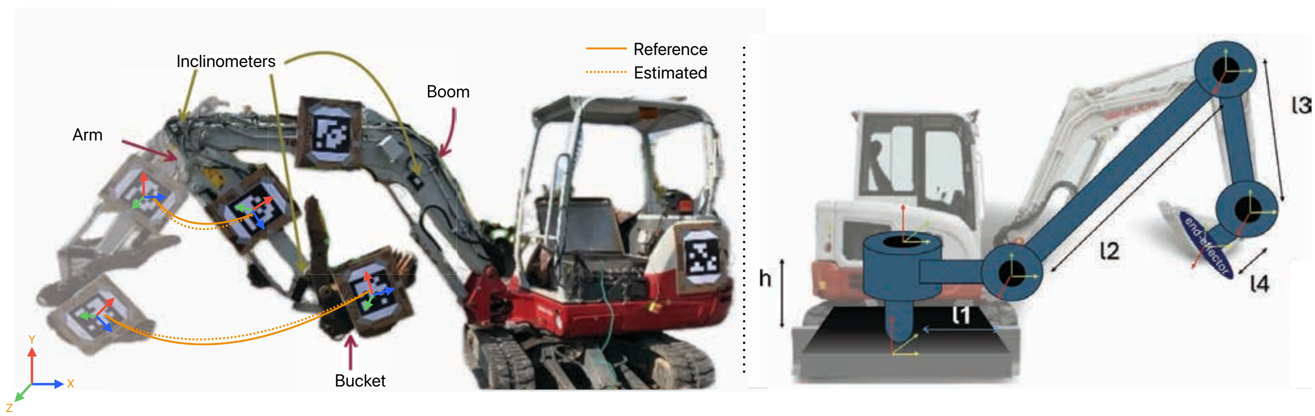

Fig. 6: Arm Pose Estimation: Estimation Evaluation (*Left*) The figure illustrates the placement of AprilTags on the excavator links(boom, arm, and bucket) and verification of IMU-based pose estimation using visually obtained ground-truth. **Joint State Estimation(*Right*)** with approximations on effective link-lengths and joint placements. The figure also illustrates the excavator's kinematic structure used for DH parameter modeling. The links l1, l2, l3 and l4 correspond to fixed link length (for offset), effective boom, arm and end effector lengths respectively

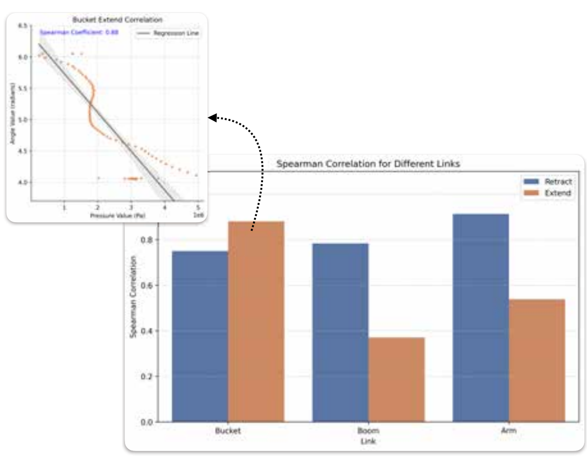

Fig. 7: Spearman correlation analysis between hydraulic pressure and joint angles for different excavator links. The inset plot highlights the bucket's extension phase, showing a strong negative correlation.

Safe planning not only mitigates risks associated with human injury, equipment damage, and environmental harm but also optimizes efficiency by enforcing constraints on key parameters. Consider the challenges excavators face: navigating through dense urban areas while avoiding collisions with buildings, digging around underground utilities without causing damage, operating in human collaborative workspace. By leveraging Control Lyapunov and Control Barrier functions (CLFs-CBFs) [23], [24], we can design reactive control-based planners that proactively respond to obstacles, ensuring safe operation well before any potential collisions occur. This approach provides formal guarantees of safety and stability, aligning with stringent industry standards.

In this work, we consider the kinematics of a 3-link planar robotic arm as the governing model to design CLF and CBF, which is given by:

$$\dot{\mathbf{P}}_e = \mathcal{J}(\boldsymbol{\theta})\dot{\boldsymbol{\theta}} \tag{2}$$

where $\mathbf{P}_e(\theta) = [x_e, y_e]$ is the set of cartesian coordinates of the end-effector position. $\boldsymbol{\theta} = [\theta_1, \theta_2, \theta_3]$ and $\dot{\boldsymbol{\theta}}$ are the joint angles and velocities respectively. Here we used the Denavit-Hartenberg (DH parameter) convention to construct the total transformation matrix from the manipulator base frame to the end-effector frame, from which the end-effector equations can be obtained. The Jacobian $\mathcal{J}(\boldsymbol{\theta})$ can be obtained by taking partial derivatives w.r.t. the joint angles. In order to ensure stability of the system, we defined a candidate Lyapunov function V in the form of two-norm distance between the target and end-effector positions, which is given by:

$$V(\mathbf{P}_e) = (x_e(\boldsymbol{\theta}) - x_f)^2 + (y_e(\boldsymbol{\theta}) - y_f)^2 \tag{3}$$

which is positive definite $\forall \mathbf{P}_e(\boldsymbol{\theta}) \neq \mathbf{P}_f$, where $\mathbf{P}_f = [x_f, y_f]$ is the target position. We adapted the exponentially stabilizing control Lyapunov function (ES-CLF) notion introduced by [25]. Furthermore, to ensure safety via collision avoidance, CBF is formulated in terms of a signed-distance function (SDF):

$$h(\mathbf{P}_e) = (x_e(\boldsymbol{\theta}) - x_f)^2 + (y_e(\boldsymbol{\theta}) - y_f)^2 - d^2 \tag{4}$$

where d is the clearance distance.

Finally, we obtained the control input $\dot{\theta}$ and corresponding trajectory by jointly optimizing the CLF and CBF using quadratic programming. The CLF-CBF-QP [26], [25], [27] formulation is given by:

$$\min_{\dot{\theta},\delta} \quad \frac{1}{2}\|\dot{\theta}\|^2 + p\delta^2 \tag{5}$$

$$\text{s.t.} \quad \dot{V} \leq -\gamma(V) + \delta \tag{6}$$

$$\dot{h} \geq -\alpha(h) \tag{7}$$

where δ is the slack variable and p is its weight. For Initial results, we run our simulation experiments with $p = 0$.

Additionally, $\alpha(.)$ and $\gamma(.)$ denote a *extended class* $\mathcal{K}_{\infty}^{e}$. In this work, we considered it as positive scalar constant.

Our preliminary simulation result is depicted in Figure 8 (Left) and the corresponding optimal safe and stable end-effector trajectory is shown in yellow. Although the proposed method offers a strong foundation for safe excavator control and planning, several practical challenges need to be addressed:

1) Simple end-effector collision avoidance is insufficient as the rigid links of the excavator arm can collide with obstacles even if the end-effector maintains a safe distance.
2) The proposed point-wise optimal control scheme results in a passive control, this often leads to undesired motion when the safety criteria are violated.
3) The optimized trajectory should account for the joint state, velocity, and actuation limits.

To address full-body collision avoidance, we develop a new CBF which accounts for the geometry of the each link.The entire link is parameterized by an ellipse whose major and minor axes are defined by length and width of the link, receptively. The center of this ellipse for each link is determined by the kinematics of the preceding links plus half the length of the current link. This elliptical representation allows us to efficiently check for collisions between the entire manipulator and obstacles in its environment. The preliminary results for full body collision avoidance in Figure 8 (Right) shows that the entire body of manipulator is able to avoid completely colliding into the point obstacle (inflated with a small radius for visualization). Synthesizing controller within QP-framework often results in undesirable trajectories. To maintain desired performance while ensuring safety, one promising direction to explore is to incorporate a trajectory re-planning strategy, as introduced in [28]. The last aforementioned challenge can be effectively handled by including additional constraints in the current formulation. However, this may lead to feasibility issues, as the constraints could conflict or limit each other. Formulating a safety definition that inherently satisfies joint limits would be a great avenue to explore further. In addition, incorporating energy-based safety constraints [29] and feasibility constraints [30] would help accommodate higher-order dynamic components.

V. Conclusion and Future Work

Engineering autonomy for excavators: Developing autonomy for excavators presents unique challenges compared to smaller mobile robots or autonomous vehicles. These massive machines operate in unstructured and dynamic construction environments, often subject to change due to the excavator's own actions. This demands robust and reliable algorithms that prioritize safety while navigating complex terrains and unpredictable obstacles. Further complicating matters is the complexity of hydraulic actuation systems commonly found in excavators. Large dead-bands, non-linear responses, and performance variations due to ambient and fluid temperatures make accurate modeling and control a significant hurdle. Our approach to building autonomy is addressing these challenges through a multi-faceted strategy currently in development: by optimizing sensor placement for maximum information gathering; exploring sensor fusion techniques; investigating the incorporation of redundancy in safety critical systems to ensure continued operation even in the event of failures; and researching algorithms that will provide formal guarantees for safe task execution.

Safe and precise excavation: The successful deployment of autonomous excavators requires a high degree of precision and safety during excavation tasks. This requirement stems from the fundamental objective of autonomous systems: to mitigate human risk and increase operational efficiency. However, achieving this precision is complicated by several factors inherent to these platforms. The substantial size and weight of these machines, combined with the non-linear and temperature-dependent behavior of hydraulic actuation systems, pose significant challenges for precise control. Thus, developing robust algorithms capable of accurately modeling and compensating for these complexities is crucial for ensuring safe and reliable autonomous excavation. To address these challenges, we have adopted a multi-pronged approach centered around simulation and real-world testing. The high-fidelity simulator, TERA [8] enables us to test and refine our algorithms in a safe and controlled virtual environment. The simulator incorporates realistic physics to accurately represent the excavator's dynamics. This helps bridge the sim-to-real gap, ensuring that our solutions are robust and transferable to real-world scenarios. Following extensive simulation testing and validation, we conduct thorough field trials to further validate and refine our algorithms, and demonstrate their efficacy.

Embodied autonomy: Finally, integrating the individual autonomy components into a cohesive system proves to be one of the most delicate tasks. This integration phase is critical because it directly impacts the excavator's ability to perform complex tasks autonomously while maintaining the highest levels of safety. Our approach leverages a modular architecture (section II), allowing for independent testing and refinement of each component before integrating them into the final system. Extensive simulation and field testing is currently underway to validate the performance of our algorithms, and we anticipate sharing final results in the near future.

References

[1] K. Dörfler, N. Hack, T. Sandy, M. Giftthaler, M. Lussi, A. N. Walzer, J. Buchli, F. Gramazio, and M. Kohler, "Mobile robotic fabrication beyond factory conditions: Case study mesh mould wall of the dfab house," *Construction robotics*, vol. 3, pp. 53–67, 2019.

[2] P. Dhamak, P. Aital, and A. Daftardar, "A comprehensive overview of Construction 4.0 technologies and their implementation in the construction industry," *Journal of Science and Technology Policy Management*, Mar. 2025.

[3] I. Okpala, C. Nnaji, O. Ogunseiju, and A. Akanmu, "Assessing the role of wearable robotics in the construction industry: potential safety benefits, opportunities, and implementation barriers," *Automation and robotics in the architecture, engineering, and construction industry*, pp. 165–180, 2022.

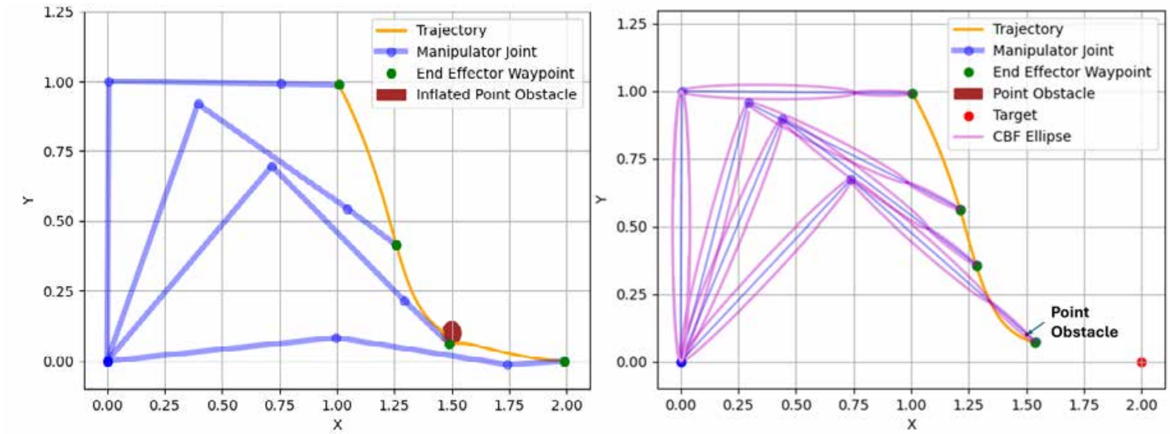

Fig. 8: Safe Planning : i) End Effector Collision Avoidance(*Left*): The Figure depicts a safe trajectory generated by optimizing with an end-effector distance -closing CLF and an end-effector safe CBF. **ii) Full Body Collision Avoidance(*Right*)**: The Figure demonstrates a trajectory generated using an end-effector distance closing CLF and a CBF that guarantees clearance from the obstacle. Preliminary results show collision avoidance.

[4] D. Jud, S. Kerscher, M. Wermelinger, E. Jelavic, P. Egli, P. Leemann, G. Hottiger, and M. Hutter, “HEAP - The autonomous walking excavator,” *Automation in Construction*, vol. 129, p. 103783, Sept. 2021.

[5] L. Zhang, J. Zhao, P. Long, L. Wang, L. Qian, F. Lu, X. Song, and D. Manocha, “An autonomous excavator system for material loading tasks,” *Science Robotics*, vol. 6, p. eabc3164, June 2021.

[6] R. Siegwart, I. R. Nourbakhsh, and D. Scaramuzza, *Introduction to Autonomous Mobile Robots*. Intelligent Robotics and Autonomous Agents series, London, England: MIT Press, 2 ed., Feb. 2011.

[7] “Takeuchi TB-235.” `https://www.takeuchi-us.com/tb235-2-specs-and-dimensions/`.

[8] C. Aluckal, R. V. K. Lal, S. Courtney, Y. Turkar, Y. Dighe, Y. Kim, J. Gemerek, and K. Dantu, “Tera: A simulation environment for terrain excavation robot autonomy,” in *In Proceedings of IEEE International Conference on Simulation, Modeling, and Programming for Autonomous Robots (SIMPAR ’25)*, (Palermo, Italy), April 2025.

[9] “Agx dynamics.” `https://www.algoryx.se/agx-dynamics/`.

[10] M. Servin, T. Berglund, and S. Nystedt, “A multiscale model of terrain dynamics for real-time earthmoving simulation,” *Advanced Modeling and Simulation in Engineering Sciences*, vol. 8, pp. 1–35, Dec. 2021. Number: 1 Publisher: SpringerOpen.

[11] “Unity sensors ROS2.” `https://github.com/Field-Robotics-Japan/UnitySensors`.

[12] B. Hofmann-Wellenhof, H. Lichtenegger, and J. Collins, *Global Positioning System*. Vienna: Springer Vienna, 2001.

[13] G. Cai, B. M. Chen, and T. H. Lee, *Unmanned Rotorcraft Systems*. Advances in Industrial Control, London: Springer London, 2011.

[14] W. Xu, Y. Cai, D. He, J. Lin, and F. Zhang, “FAST-LIO2: Fast Direct LiDAR-Inertial Odometry,” *IEEE Transactions on Robotics*, vol. 38, pp. 2053–2073, Aug. 2022. Conference Name: IEEE Transactions on Robotics.

[15] C. Campos, R. Elvira, J. J. G. Rodríguez, J. M. M. Montiel, and J. D. Tardós, “ORB-SLAM3: An Accurate Open-Source Library for Visual, Visual–Inertial, and Multimap SLAM,” *IEEE Transactions on Robotics*, vol. 37, pp. 1874–1890, Dec. 2021. Conference Name: IEEE Transactions on Robotics.

[16] T. Shan, B. Englot, D. Meyers, W. Wang, C. Ratti, and D. Rus, “LIO-SAM: Tightly-coupled Lidar Inertial Odometry via Smoothing and Mapping,” in *2020 IEEE/RSJ International Conference on Intelligent Robots and Systems (IROS)*, pp. 5135–5142, Oct. 2020. ISSN: 2153-0866.

[17] C. Zheng, Q. Zhu, W. Xu, X. Liu, Q. Guo, and F. Zhang, “FAST-LIVO: Fast and Tightly-coupled Sparse-Direct LiDAR-Inertial-Visual Odometry,” Mar. 2022. arXiv:2203.00893 [cs].

[18] Y. Turkar, T. C. Jr, C. Aluckal, and K. Dantu, “Learning Visual Information Utility with PIXER,” Sept. 2024. arXiv:2409.13151 [cs].

[19] K. Singh, C. Adhivarahan, and K. Dantu, “L-DYNO: Framework to Learn Consistent Visual Features Using Robot’s Motion,” in *2024 IEEE International Conference on Robotics and Automation (ICRA)*, pp. 17522–17528, May 2024.

[20] C. A. C. A. K. D. Yash Turkar, Pranay Meshram, “Empir3d: Multi-dimensional point cloud quality assessment,” 2024.

[21] R. T. Robin Deits, “Efficient Mixed-Integer Planning for UAVs in Cluttered Environments,”

[22] E. Olson, “Apriltag: A robust and flexible visual fiducial system,” in *2011 IEEE International Conference on Robotics and Automation*, pp. 3400–3407, 2011.

[23] A. D. Ames, S. Coogan, M. Egerstedt, G. Notomista, K. Sreenath, and P. Tabuada, “Control Barrier Functions: Theory and Applications,” in *2019 18th European Control Conference (ECC)*, (Naples, Italy), pp. 3420–3431, IEEE, June 2019.

[24] A. Alan, A. J. Taylor, C. R. He, A. D. Ames, and G. Orosz, “Control Barrier Functions and Input-to-State Safety With Application to Automated Vehicles,” *IEEE Transactions on Control Systems Technology*, vol. 31, pp. 2744–2759, Nov. 2023.

[25] M. Desai and A. Ghaffari, “CLF-CBF Based Quadratic Programs for Safe Motion Control of Nonholonomic Mobile Robots in Presence of Moving Obstacles,” in *2022 IEEE/ASME International Conference on Advanced Intelligent Mechatronics (AIM)*, (Sapporo, Japan), pp. 16–21, IEEE, July 2022.

[26] W. Li, D. Zhang, G. Shao, and Z. Wu, “Safety control for a 2-DOF planar manipulator based on penalty Quadratic Program,” in *2024 36th Chinese Control and Decision Conference (CCDC)*, (Xi’an, China), pp. 586–591, IEEE, May 2024.

[27] J. Huang, X. Chi, Z. Liu, and H. Su, “Whole-body Dynamic Collision Avoidance with Time-varying Control Barrier Functions,” in *2024 36th Chinese Control and Decision Conference (CCDC)*, (Xi’an, China), pp. 5149–5154, IEEE, May 2024.

[28] Y. Kim, C. R. He, and T. Singh, “Control Barrier Function based Energy optimal Obstacles Avoidance for Point-to-Point Maneuvers,” *IFAC-PapersOnLine*, vol. 58, no. 28, pp. 857–862, 2024.

[29] A. Singletary, S. Kolathaya, and A. D. Ames, “Safety-Critical Kinematic Control of Robotic Systems,” *IEEE Control Systems Letters*, vol. 6, pp. 139–144, 2022.

[30] W. Xiao, C. A. Belta, and C. G. Cassandras, “Sufficient conditions for feasibility of optimal control problems using Control Barrier Functions,” *Automatica*, vol. 135, p. 109960, Jan. 2022.